

# Comparison of Frame Material with Consideration to Static Load Deflection

Author: Glenn Petersen

ME 404 – Dr. Scott Hazelwood

## Abstract

This analysis provides insight into the comparison of bicycle frame material between steel, AISI 4130 or Chromoly, and aluminum, 7005 – T6. The results show a good relationship with the hand calculations as well as a selection of mesh that optimizes convergence and computational run time and effort. A noted result of the 3D stand analysis for the steel frame was a bottom bracket averaged deflection in the U2 direction of 0.1629 mm. The aluminum frame showed a 0.1735 mm deflection average. Further, a comparison of the ratio of deflection to weight, provides insight on the relative gain or loss in the selection of either steel or aluminum on the relative feel and weight of the bicycle frame; an overall 30% increase in deflection to weight ratio for aluminum frame from steel. The overall analysis saw errors related to the Tie-constraint function of Abaqus which originated from improper ‘master-slave’ surface relationship and multiple reference of the same ‘slave’ surface which was remedied with a reorganization of the constraints. The thin wall nature of bicycle tubing provided easy opportunity of distorted elements without refining the mesh beyond reasonable computational time and resources.

## Introduction

While steel or aluminum may appear perfectly ridged to the laymen, an avid rider is able to feel the difference, even if the weight and geometry are comparable. In consideration to custom bikes, steel butted tubing is still very popular as it is easier to weld and does not require post welding heat treatment. However, provided the same geometry and loading, how much different will a bike made from aluminum feel in comparison to one made from steel?

Primary areas of deflection will be where the road profile is transmitted to the rider, this is transvers deflection of the chain stays and compression column bending of the seat stays. Another area with notable deflection will be in the fork and consequently a potential rotation of the head tube due to its own distortion and related compression of the top tube and extension of the down tube. Further, a common point is the bottom bracket tube, located at the intersection of the chain-stays, seat tube, and down tube, shown in Figure 1.

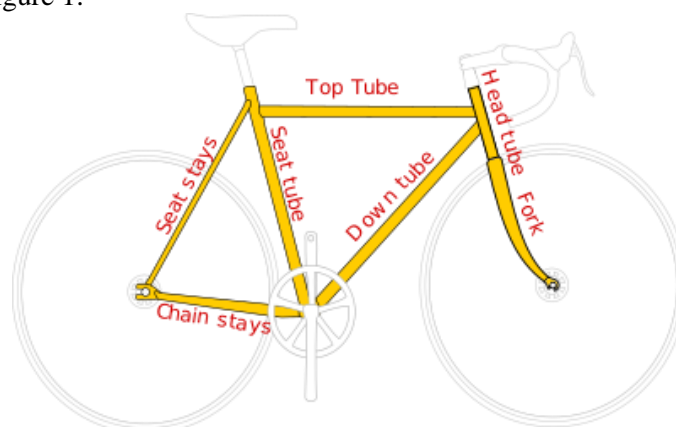


Figure 1. Bicycle frame tubes labeled.

The results of this analysis will provide insight into material selection with consideration to rigidity and weight. This will allow better decisions to be made about the desired material for the costs or benefits in manufacturing effort and material costs. The primary beneficiaries will be members of Cal Poly Bike Club and myself provided with this better understanding towards material selection.

## Model Development

I initially designed a bicycle using a 2D CAD program called BikeCAD for a gravel bike; a heavier duty road bike that will encounter a bumpier surface where flex of frame in combination to durability and rigidity are important factors. The specified geometry is shown below in Figure 2. I chose to simplify the possible model by not including extremely complex tubing cross sections and keeping any bends (which are very common on custom and mass-produced bicycles) to within a single plane. To keep the bicycle model realistic, I selected tubes that could be used to build up both the steel and aluminum frame, noted in Appendix 1.

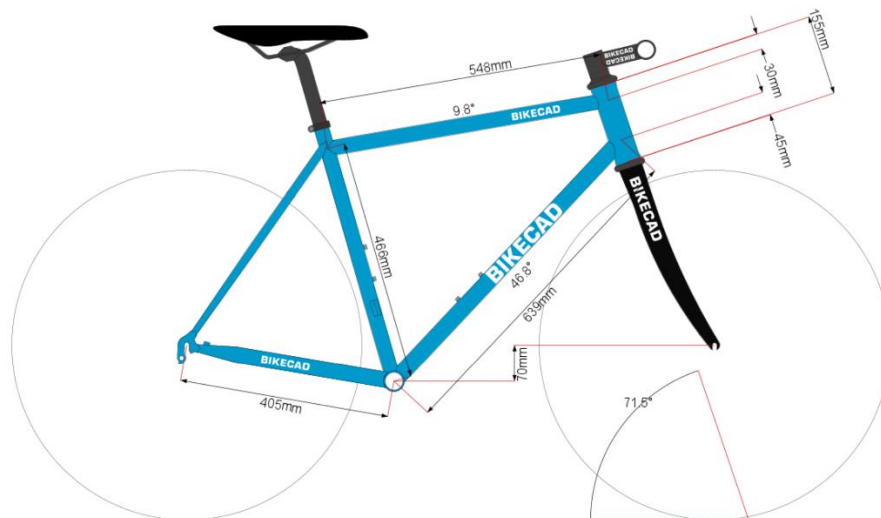


Figure 2. BikeCAD model of bicycle frame with key dimensions labeled.

With the basic 2D geometry figured out and tubes for each frame selected, I next created a 3D model, shown in Figure 3a and 3b. Some considerations needed here are the rear axle width and rear dropout type. To keep it as general as possible as there is not one type of dropout, I decided to utilize a basic cylinder shape. Another simplification made is the exclusion of the fork, as any fitting fork can go in either frame, I deemed it not within the confines of this analysis as I am specifically looking at the frame but not all the components which can be attached and ultimate would affect the 'feel' of the bike.



Figure 3. a) Aluminum frame shown on the left, b) steel frame shown in right. Note the use of cylindrical rear axle dropouts.

Bringing the 3D CAD models into Abaqus was not a particularly simple process, the primary issue being the assembly of the tubes within Abaqus. I modeled the frame in Solidworks with each tube being non-merged with the connecting parts and then imported a .STEP file as individual parts. Each part then had to be constrained to each other via tie constraints on each contacting surface. This leads to a ‘master-slave’ relationship which has mesh consequences described in the Mesh Development section.

During the process of selecting the tubes for an aluminum frame and steel frame, the notable differences found are in the overall tube diameter and wall thickness; with the aluminum frame being larger in both regards. This leads to the alloy selection, I selected tubes made from aluminum 7005-T6 alloy due to the advertised benefits of not requiring a post weld heat treatment process to remove common brittle behavior seen in other aluminum alloys. This is favorable for our beneficiaries who are bike builders. In consideration to the steel frame the most common and popular alloy is AISI 4130, or Chromoly. A summary of technical material properties is shown in Table 1. Since the geometry of the frame is defined in millimeters, the Modulus of Elasticity must be defined in mega-Pascals in Abaqus.

Table 1. Material Properties Table

Material	Modulus of Elasticity	Poisson Ratio	Density
	[ GPa ]	[ - ]	[kg/m <sup>3</sup> ]
AISI 4130 (chromoly)	205	0.29	7850
Aluminum 7005 – T6	70	0.33	2900

Now with each model having defined geometry and material, the loading condition can be defined. Provided other complexities in this model a static loading condition to provide a general perspective of the compliancy of the frame is selected. This leads to a standard analysis and deflection results. Shown in Figure 4, the rear axle inner surfaces are constrained positionally, allowing for free rotation in any direction; similarly, the bottom of the head tube surface and 15 mm of the inner housing surface is also constrained positionally with free rotation. This is to mimic the contact from the bottom headset cup on the head tube.



Figure 4. Loading and boundary constraints for both aluminum (left) and steel (right) models. The orange arrows represent boundary constraints

Since a fork is not considered in this model, another simplification made is not constraining the upper headset cup race of the head tube; this is reasonable as the primary load path is through the bottom cup race with a static compressive load at the seat tube. The potential excess torsion of the head tube is a factor that is being overlooked in this analysis for simplicity and times' sake, however, this is an opportunity for further investigation.

The purple arrows shown in Figure 4 represent the loading on the model. The primary definition is a 2400 N load on the top surface of the seat tube, this is represented in the model as a pressure on that surface. For the steel model this results in a pressure load of 45.47 MPa, and 13.88 MPa for the aluminum model.

### Mesh Development and Mesh Convergence

Since the scale of each model is the same, as well as the tubes being similar wall thicknesses, I developed the mesh for both models for just the steel model. Then results were applied to the aluminum model. Throughout the model quadratic tetrahedral elements were utilized, specifically C3D10. Approaching this 3D model as a solid homogenous body, tetrahedral elements were the best approach with consideration to the thin walls as well as a combination of bending and compression possibilities. As previous mentioned in the Model Development section, consideration to the tie-constraint relationships had to be accounted for which requires the 'slave' surface have a higher mesh density. This had to be planned accordingly and changed for each tube appropriately as I conducted a mesh convergence analysis. A table of the global seed size for each tube in each round of the mesh convergence analysis is noted in Table 2.

Table 2. Global seed size for each round of mesh convergence for each tube, in mm.

	Round 1	Round 2	Round 3	Round 4
Seat Tube	3	4	5	3.5
Seat Stay	2	3	4	2.5
Chain Stay	2	3	4	2.5
Down Tube	2	3	4	2.5
Bottom Bracket	1	2	3	1.5
Rear Axle	3	4	5	3.5
Head Tube	3	4	5	3.5
Top Tube	2	3	4	2.5

To retrieve the deflection of the bottom bracket I did not care about a specific region of the bottom bracket but more the bottom bracket in its entirety. To do this took the U, U2 deflection values from Abaqus to an .rpt file, nodes selected shown in Figure 5. From them I processed the data leaving the multiple references of the node and deflection value, but I still need to remove the duplicate values (from the data reference to each connecting element) to get an appropriate average for the bottom bracket as a whole. I wrote a MATLAB® script to do this and find the average deflection for the bottom bracket. Code is attached in Appendix 2.

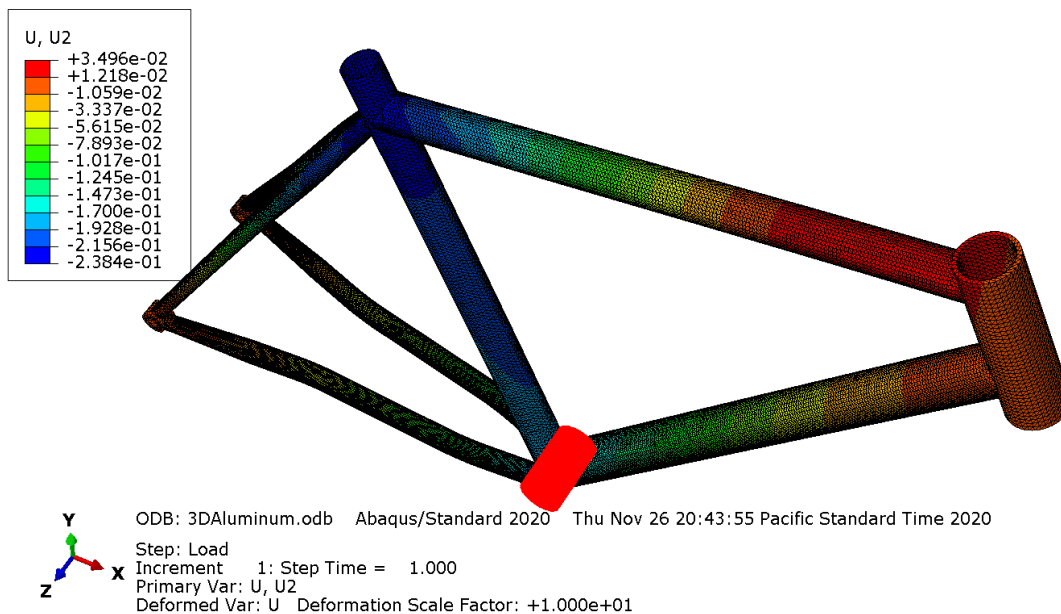


Figure 5. The red bottom bracket is all nodes of the bottom bracket being highlighted. The deflection in the U2 direction of these nodes are utilized to find the average deflection of the bottom bracket.

Running the analysis for each defined round provided enough deflection measurements of the bottom bracket deflection in the U2 direction to be taken, results in Table 3 and graphed in Figure 6. Note the flat line of bottom bracket deflection as the mesh is refined showing that extra refined mesh does not result in notable difference of deflection modeled.

Table 3. Results of mesh convergence for steel model

Global Seed Size [ mm ]	Total Number of Variables [ - ]	Deflection of Bottom Bracket [ mm ]	Wall Clock Time [ s ]
Round 1	2778506	-0.1644	1000
Round 4	1694540	-0.1634	454
Round 2	1187490	-0.1629	328
Round 3	665105	-0.2029	57

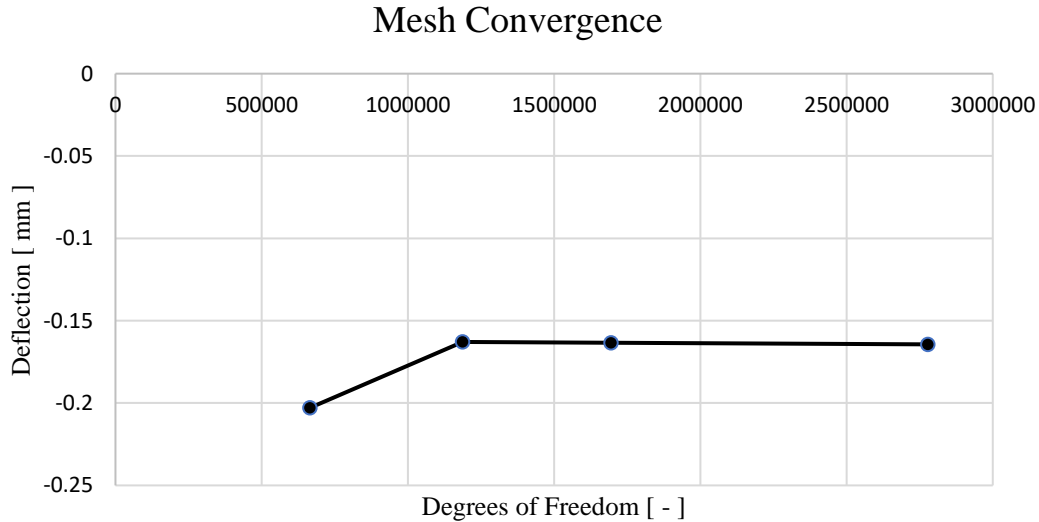


Figure 6. Plot of bottom bracket deflection in the U2 direction showing a flat line after Round 2 global seed sizes.

Utilizing these results, I was able to confirm that it was unnecessary to refine the mesh further than what is defined for each tube for Round 2 in Table 2. This save a significant amount of computational time and resources as noted by the Wall Clock Time retrieved from the job .DAT file.

At this selected mesh definition, the steel model has a total 197,239 elements and 1,187,490 degrees of freedom. For the aluminum model, the same mesh definition is used; however, the chain stay values were refined due to an over constraint error of the tie-constraints due to proximity to the seat tube, resulting in a switch of ‘master-slave’ definition requiring the chain stay mesh density to be decreased to 1.9 mm global seed size at the surface while keeping the majority of the chain stay at the 3 mm global seed size. Therefore, the aluminum model has a total 232,556 elements and 1,343,586 degrees of freedom.

Although I achieved mesh convergence, the wall thickness of the tubes proved to be an issue with mesh quality. Since the wall thickness was so small, relative to the overall diameter, elements often did not pass the min/max angle and aspect ratio criteria. However, the deflection results in comparison to the hand calculation estimate proved the model was not wildly incorrect.

## Analysis

The analysis performed for all rounds and models is Abaqus Standard. As I was looking for static loading deflection of the frame, no dynamic simulation was required. The only error I encountered while running

my analysis was an over constraint on slave surfaces for the tie constraint. This over constraint occurred when two or more tie constraints utilized the same surface as a slave surface, more specifically the nodes on the surface. This was resolved by correcting the slave-master order for the tie constraint. During all jobs, the tie-constraint adjusts the nodes on the surface selected appropriately to ensure a solid tie constraint is made; however, due to the high mesh density I repeatedly got a warning that not all adjusted nodes were being printed in the .DAT file since there were too many, so this warning is more of a notification that does not have any implication on the results of the model.

Due to the high volume of nodes on the surfaces utilized for constraints, a generalized surface much larger than the exact contact path were selected, this led to a large number of nodes not being able to be adjusted to match as they were outside the adjustable range; moreover, it would not have made sense to adjust them since they were so far away from the contact patch. The other nodal warning that occurred on all jobs was several distorted elements, this is from the thin wall tubing resulting in elements not passing the suggested isoparametric angles. However, the mesh size required to improve this results in a drastic increase total number of elements and subsequently computational time and effort. The mesh convergence shows that although there are distorted elements, they are not affecting the results as the reduction of distorted elements does not show a large change in deflection.

## Results

In consideration towards the objective of comparing a steel frame to an aluminum frame. I created a value that is the ratio of deflection to frame weight, shown in Table 4. This shows that although they have different deflection of the bottom bracket and total weights of the frame, they have similar deflection to weight, but steel is still stiffer per weight than aluminum.

Table 4. Results from FEA models and hand calculations. Hand calculation are shown in Appendix 3.

Model	Deflection [ mm ]	Weight [ g ]	Deflection/Weight [ mm/g ]
3D Steel	0.1629	1651.77	9.86E-05
3D Aluminum	0.1735	1242.42	1.40E-04
3D Steel HC	0.45	-	-

Looking at the total frame and where deflection is scene, note Figure 7 and Figure 8. Each shows a similar pattern in deflection of the frame with noted increase in deflection for the aluminum frame. We can consider breaking the bicycle into 3 main regions: the center where the bottom bracket and seat tube are located; the intermediary, the tubes connecting the center to the outside constraints (down tube, top tube, seat and chain stays); and the outside constraints, head tube and rear axle dropouts. The outside constraints show the least deflection, which makes sense since this is where the constraints holding position are located. The center shows the most deflection, the darkest blue, as this is where the load is applied and is the farthest away from where the constraints are located. Then the intermediary region shows the gradient from the outside to the center for deflection, showing a large amount of energy being dissipated through these tubes.

Further, consider Figure 9; each bottom bracket shows a similar deflection pattern with the one counter intuitive result of the bottom have of the tube having positive upward deflection. This most likely due to the lack of support from the internal bearing assembly and crank that would be present in an assembled bicycle. Further, no loading is provided at the cranks, as there would be in most riding conditions.



Figure 7. Side profile image of 3D steel model utilizing round 2, from Table 2, global seed sizes.

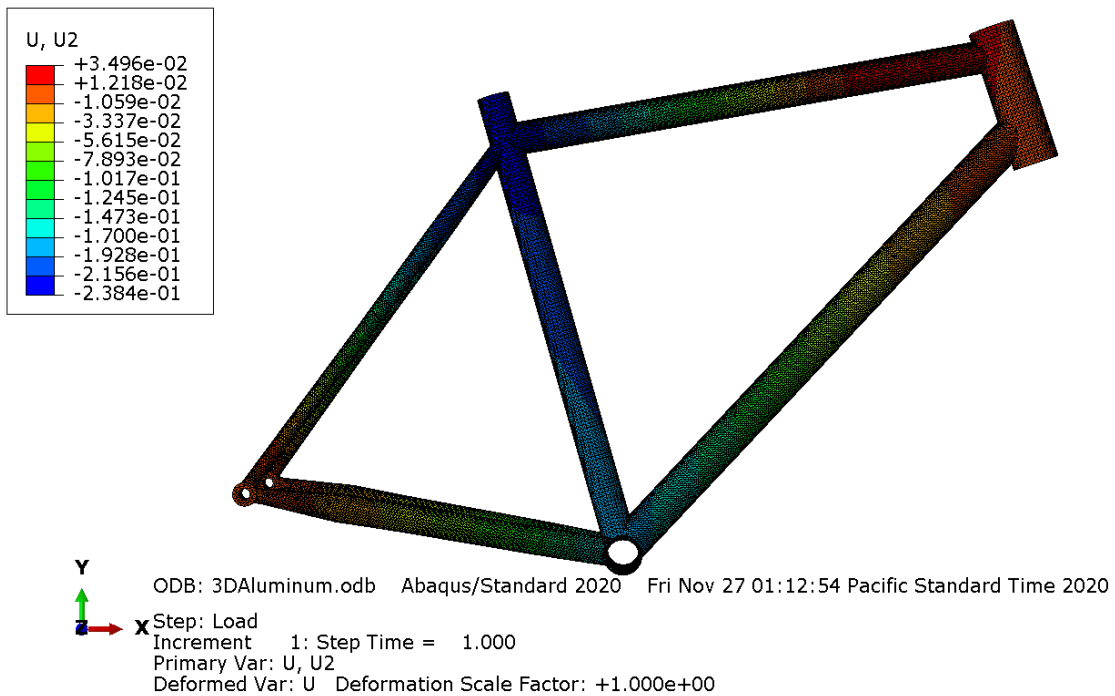


Figure 8. Side profile image of 3D aluminum model utilizing round 2, from Table 2, global seed sizes.

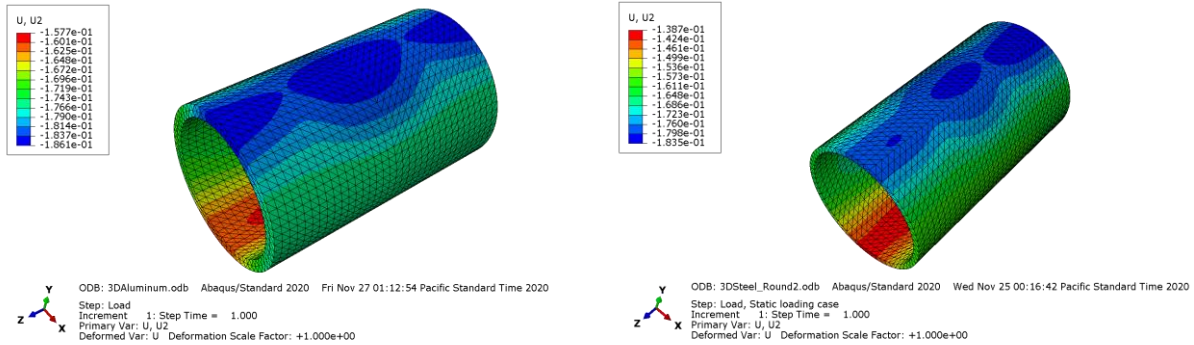


Figure 9. Close up of only bottom bracket U2 deflection for aluminum (left) and steel (right).

## Discussion

The results of this analysis provide implications into the decision of custom manufacturing of bicycles. With the noted difference in stiffness versus weight, we see a small benefit in stiffness per weight if we consider being stiffer is better in the steel frame. Now this can be beneficial or not depending on the desired use and feel of the frame. However, this also provides a perspective on the magnitude of the theoretical gain, in either direction, for the manufacturer. This allows the designer to weigh the benefit of stiffness per weight one way or the other, with the other manufacturing consequences with either a steel or aluminum frame. If the design consideration is purely a lighter frame, aluminum should be considered as a good option for frame material; however, recognition of a flexier frame needs to be made and potentially another material should be utilized if the stiffness is highly desired as well. Conversely, of the two materials, steel provides greater stiffness with a cost of total frame weight.

This analysis provides a peak into the resolutions made however, there are many factors that are not account for which can and will affect the deflection under a static load. Primarily, tube cross-sectional shape and bends that are introduced or the lack of bends introduced. These are factors that are assumed to be relative constant between the steel and aluminum frame, provided the availability of the tubes in the market. These factors alone could constitute their own analysis on their impacts on the same implications made previously.

Consider the results in Table 4. Note the similarity from the aluminum and steel frame simulations from Abaqus FEA standard analysis, with noted large, relative, difference in comparison to the hand calculation results. The primary differences introduced between the two approaches, is the hand calculations only consider a straight-line truss structure with no consideration to bending only axial compression and tension. The FEA model does account for bending as well as axial tension and compression which leads to a lower deflection value as there is another factor which provides stiffness to the frame. This leads to the relative approval of the FEA results with the hand calculations as they do not differ by an order of magnitude.

Overall, the results of this project and FE method analysis have provided good results and insight into the question of steel or aluminum. The common notion is that aluminum is lighter, which is true, but it is also softer and may not provide the same ‘nippy’ feel steel could provide. This also confirms the notion that aluminum is not plainly better than steel, there are benefits and countering cons to each material and their use in a frame. Looking towards a revamp of this analysis, I would try to consider the other factors at play: tube shape, the influence of chain stay and seat stay bends, a dynamic analysis on the vibratory component (consider riding over gravel).

## Conclusion

This analysis provides insight into the function and influence of material on the static deflection of a bicycle. The results show the less dense aluminum does provide a lighter frame; however, at the cost of more deflection. Inversely, a steel frame provides less deflection, but at the cost of a heavier frame. To try and compare these two, a ratio of deflection to weight is created and shows only a roughly 30% increase in deflection per weight for aluminum over steel. However, this is not a bad or good thing, it is just insight into the decision process of selecting a frame material.

## Appendices

- 1) Tube Selection
- 2) MATLAB® code for deflection averaging
- 3) Hand calculation for steel frame deflection

## Appendix 1 – Tube Selection

### Steel Frame

Head Tube - HT2014: Steel 44 mm, Single, 150 mm, 1-7/8" x 50 mm OD from Paragon Machine Works (<https://www.paragonmachineworks.com/frame-building-parts/headtubes/steel/ht2014-44-mm-headtube.html>)

Down Tube – Columbus Zona 29er Top/Down Tube - 31.7 Dia. - .7/.5/.7 - Length = 650 from Framebuilder Supply (<https://framebuildersupply.com/collections/down-tubes/products/columbus-zona-29er-top-tube-31-7-dia-7-5-7-length-650>)

Top Tube – Columbus Zona Top Tube - 28.6 Dia. - .7/.5/.7 - Length = 600 from Framebuilder Supply (<https://framebuildersupply.com/collections/top-tubes/products/columbus-zona-top-tube-28-6-dia-7-5-7-length-600>)

Seat Tube – Columbus Cromor Single Butted Seat Tube - 28.6 Dia. - .9/.6 - Length = 640 from Framebuilder Supply (<https://framebuildersupply.com/collections/seat-tubes/products/columbus-cromor-single-butted-seat-tube-28-6-dia-9-6-length-640>)

Seat Stays – Columbus Zona Cyclocross S-Bend Seat Stays - 16 OD - .7 Wall - Length = 560 from Framebuilder Supply (<https://framebuildersupply.com/collections/seat-stays/products/columbus-zona-cross-s-bend-seatstays-16-od-7-wall-length-560>)

Chain Stays – Columbus Life Butted Cyclocross S-Bend Chainstays - Oval/Round - 24 OD - .8/.6 Wall - Length = 410 from Framebuilder Supply (<https://framebuildersupply.com/collections/chain-stays/products/columbus-life-butted-cx-s-bend-chainstays-oval-round-24-od-7-5-wall-length-410>)

Bottom Bracket – Bottom Bracket Shells - ISO Threaded - 69mm, 74mm, 101mm - 38.1mm OD from Framebuilder Supply (<https://framebuildersupply.com/collections/lugless-bb-shells/products/bottom-bracket-shells-69mm-74mm-101mm-38-1mm-od-iso>)

### Aluminum Frame

Head Tube – NOVA AL7005 HT 50.8MM X 3.7 X 200MM from Nova Cycle Supply (<https://www.cycle-frames.com/NOVA-50.8mm-x-3.7-200mm.html>)

Down Tube – NOVA 42 X 700 DOWN TUBE T-6 from Nova Cycle Supply ([https://www.cycle-frames.com/NOVA-42-X-700-DOWN-TUBE-T-6.html?category\\_id=1125](https://www.cycle-frames.com/NOVA-42-X-700-DOWN-TUBE-T-6.html?category_id=1125))

Top Tube – 35 X 610 7005 TOP TUBE from Nova Cycle Supply ([https://www.cycle-frames.com/35-X-610-7005-TOP-TUBE.html?category\\_id=1125](https://www.cycle-frames.com/35-X-610-7005-TOP-TUBE.html?category_id=1125))

Seat Tube – 35 X 500 7005 SEAT TUBE from Nova Cycle Supply ([https://www.cycle-frames.com/35-x-500-7005-SEAT-TUBE.html?category\\_id=1125](https://www.cycle-frames.com/35-x-500-7005-SEAT-TUBE.html?category_id=1125))

Seat Stays – NOVA AL7005 MTB"S"BEND SEATSTAY from Nova Cycle Supply ([https://www.cycle-frames.com/NOVA-AL7005-MTB-SEAT-STAY-S-BEND.html?category\\_id=964](https://www.cycle-frames.com/NOVA-AL7005-MTB-SEAT-STAY-S-BEND.html?category_id=964))

Chain Stays – NOVA T-6 AL7005 RD CHAINSTAY WITH S BEND from Nova Cycle Supply ([https://www.cycle-frames.com/NOVA-T-6-AL7005-RD-Chainstay-with-S-BEND.html?category\\_id=1556](https://www.cycle-frames.com/NOVA-T-6-AL7005-RD-Chainstay-with-S-BEND.html?category_id=1556))

Bottom Bracket – NOVA 7005 AL BB ROAD SHELL 69MM WIDE THREADED from Nova Cycle Supply ([https://www.cycle-frames.com/NOVA-7005-AL-BB-ROAD-SHELL-69mm-THREADED.html?category\\_id=957](https://www.cycle-frames.com/NOVA-7005-AL-BB-ROAD-SHELL-69mm-THREADED.html?category_id=957))

## Appendix 2 – MATLAB® code for average bottom bracket deflection values

```
clear;  
close all;  
clc
```

### Import Data

```
r1 = importdata('3Dsteel_round1_edited.xlsx');  
r2 = importdata('3Dsteel_round2_edited.xlsx');  
r3 = importdata('3Dsteel_round3_edited.xlsx');  
r4 = importdata('3Dsteel_round4_edited.xlsx');  
a1 = importdata('3Daluminum_edited.xlsx');
```

### Round 1

#### Remove Duplicates

Find each duplicate initial value index, ia

```
[C, ia, ic] = unique(r1(:,1));  
r1_def = r1(ia,2);
```

#### Find Average Value

```
r1_def_ave = mean(r1_def)
```

```
r1_def_ave = -0.1644
```

### Round 2

#### Remove Duplicates

Find each duplicate initial value index, ia

```
[C, ia, ic] = unique(r2(:,1));  
r2_def = r2(ia,2);
```

#### Find Average Value

```
r2_def_ave = mean(r2_def)
```

```
r2_def_ave = -0.1629
```

### Round 3

## Remove Duplicates

Find each duplicate initial value index, ia

```
[C, ia, ic] = unique(r3(:,1));  
r3_def = r3(ia,2);
```

Find Average Value

```
r3_def_ave = mean(r3_def)
```

```
r3_def_ave = -0.2029
```

Round 4

## Remove Duplicates

Find each duplicate initial value index, ia

```
[C, ia, ic] = unique(r4(:,1));  
r4_def = r4(ia,2);
```

Find Average Value

```
r4_def_ave = mean(r4_def)
```

```
r4_def_ave = -0.1634
```

Aluminum 1

## Remove Duplicates

Find each duplicate initial value index, ia

```
[C, ia, ic] = unique(a1(:,1));  
a1_def = a1(ia,2);
```

Find Average Value

```
a1_def_ave = mean(a1_def)
```

```
a1_def_ave = -0.1735
```

Appendix 3 – Hand Calculations of steel frame deflection

TUBE CROSS SECTIONAL SIZES

ALL UNITS IN mm  
UNLESS OTHERWISE  
SPECIFIED

DT:  $\phi 31.7$  - 0.7 / 0.5 / 0.7

WALL THICKNESS

$\Rightarrow$  AVERAGE  $T = 0.6$

$$\Rightarrow A_{DT} = \frac{\pi}{4} (0.0317^2 - 0.0305^2) \text{ m}^2$$

$$A_{DT} = 0.0000986 \text{ m}^2$$

TT:  $\phi 28.6$  - 0.7 - 0.5 - 0.7

$\Rightarrow T = 0.6$

$$\Rightarrow A_{TT} = \frac{\pi}{4} (0.0286^2 - 0.0274^2) \text{ m}^2$$

$$A_{TT} = 0.0000528 \text{ m}^2$$

SS:  $\phi 16-12.5$   $t = 0.7$

$\phi \approx 14$

$$A_{SS} = \frac{\pi}{4} (0.014^2 - 0.0126^2) \text{ m}^2$$

$$A_{SS} = 0.0000292 \text{ m}^2$$

ST:  $\phi 28.6$  -  $\phi 27.4$  ID

$$A_{ST} = \frac{\pi}{4} (0.0286^2 - 0.0274^2) \text{ m}^2$$

$$A_{ST} = 0.0000528 \text{ m}^2$$

CS:  $\phi 28$  OTHER END IS ROUND  
ASSUME CONS.

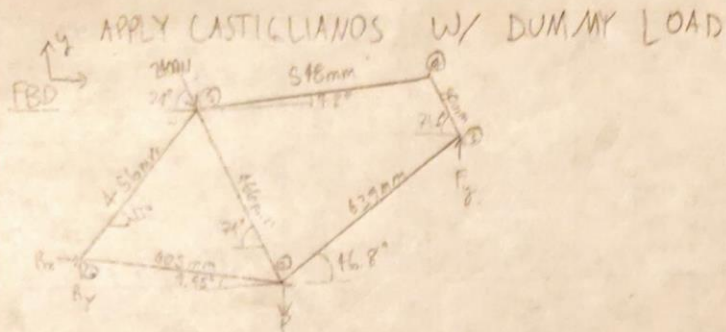
$$A_{CS} = \pi \left( \frac{0.028 \cdot 0.014}{2} - \frac{0.026 \cdot 0.026}{2} \right) \text{ m}^2$$

$$A_{CS} = 0.0001436 \text{ m}^2$$

HT:  $10\phi 45$  -  $00\phi 47.6$

$$A_{HT} = \frac{\pi}{4} (0.0476^2 - 0.045^2) \text{ m}^2$$

$$A_{HT} = 0.0001891 \text{ m}^2$$



SOLVE FOR REACTIONS

$$\sum M_R = 0$$

$$-2400 \sin 74 (456 \cos 55) - 2400 \cos 74 (456 \sin 55) + F_y (639 \cos 46.8 + 405 \cos 99.95) - P (405 \cos 99.95) = 0$$

$$F_y (836.334) = 850508.5 + 398.908 P$$

$$F_y = 1016.948 + 0.477 P \quad N$$

$$\sum F_x = 0$$

$$2400 \cos 74 + R_x = 0$$

$$R_x = -661.5297 \text{ N}$$

$$\sum F_y = 0$$

$$-2400 \sin 74 + R_y + 1016.948 + 0.477 P - P = 0$$

$$R_y = 1290.08 + 0.523 P$$

JOINT ①



$$\sum F_x = 0$$

$$-661.5297 + F_5 \cos 55 + F_2 \cos 9.95 = 0$$

$$F_2 = -0.5823 F_5 + 671.63 \quad (1)$$

$$\sum F_y = 0$$

$$R_y + F_5 \sin 55 - F_2 \sin 9.95 = 0$$

$$1290.08 + 0.523P + F_5 \sin 55 - F_2 \sin 9.95 = 0$$

$$F_5 = \frac{-1290.08 - 0.523P}{\sin 55} + \frac{F_2 \sin 9.95}{\sin 55}$$

$$F_5 = -1574.897 - 0.6384P + 0.211 F_2$$

$$= -1574.897 - 0.6384P + 0.211(-0.5823 F_5 + 671.63)$$

$$= -1574.897 - 0.6384P - 0.12286 F_5 + 141.7139$$

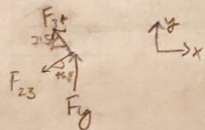
$$1.12286 F_5 = -1433.183 - 0.6384P$$

$$F_5 = \underline{-1276.362 - 0.5685P} \quad (C)$$

$$\Rightarrow F_2 = -0.5823(-1276.362 - 0.5685P) + 671.63$$

$$F_2 = \underline{1414.856 + 0.331P} \quad (T)$$

JOINT ③



$$\sum F_x = 0$$

$$-F_{3+} \cos 71.5 - F_{23} \cos 46.8 = 0$$

$$F_{3+} = -2.1573 F_{23}$$

(CONT)

$$\Sigma F_y = 0$$

$$F_y - F_{23} \sin 16.8 + F_{34} \sin 71.5 = 0$$

$$1016.948 + 0.477P - F_{23} \sin 16.8 - 2.1573 F_{23} \sin 71.5 = 0$$

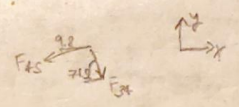
$$F_{23} = \frac{1016.948}{2.7747} + \frac{0.477P}{2.7747}$$

$$F_{23} = 366.496 + 0.172P \quad (T)$$

$$F_{34} = -2.1573 (366.496 + 0.172P)$$

$$F_{34} = -790.6418 - 0.371P \quad (C)$$

JOINT ④



$$\Sigma F_x = 0$$

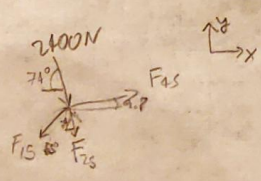
$$-F_{45} \cos 9.8 + F_{34} \cos 71.5 = 0$$

$$F_{45} = -0.322 F_{34}$$

$$F_{45} = -0.322 (-790.6418 - 0.371P)$$

$$F_{45} = 254.589 + 0.119P \quad (T)$$

JOINT ⑤



$$\Sigma F_x = 0$$

$$F_{45} \cos 9.8 - F_{15} \cos 55 + F_{25} \cos 74 + 2400 \cos 74 = 0$$

$$F_{25} = \frac{-1}{\cos 74} (2400 \cos 74 - (-1276.362 - 0.5685P) \cos 55 + ((254.589 + 0.119P) \cos 9.8)$$

(CONT)

$$F_{23} = -2400 + 2655.994 - 1.18299P - 910.1597 - 0.425P$$

$$F_{23} = +5966.154 - 1.608P \quad (c)$$

MEMBER	F FORCE [N]	dF/dP	F <sub>i</sub> (P=0)	L (m)	A (m <sup>2</sup> )
(1) 1-2	1414.856 + 0.331P	0.331	1414.856	0.405	(0.0001436)2
(2) 1-5	-1276.362 + 0.5665P	-0.5665	-1276.362	0.456	(0.000292)2
(3) 2-5	-5966.154 + 1.608P	-1.608	-5966.154	0.466	0.0000528
(4) 4-5	254.589 + 0.119P	0.119	254.589	0.548	0.0000528
(5) 3-4	-790.6418 - 0.371P	-0.371	-790.6418	0.08	0.0001891
(6) 2-3	366.496 + 0.172P	0.172	366.496	0.639	0.0000586

$$E = 205 \times 10^9 \text{ Pa}$$

$$\Delta = \sum_1^6 F_i \left( \frac{dF_i}{dP} \right) \frac{L_i}{AE}$$

$$= \frac{1}{205 \times 10^9} \left[ 1414.856 \left( 0.331 \right) \left( \frac{0.405}{(0.0001436)^2} \right) + (-1276.362) \left( -0.5665 \right) \left( \frac{0.456}{(0.000292)^2} \right) \right. \\ \left. + (-5966.154) \left( -1.608 \right) \left( \frac{0.466}{0.0000528} \right) + (254.589) \left( 0.119 \right) \left( \frac{0.548}{0.0000528} \right) \right. \\ \left. + (-790.6418) \left( -0.371 \right) \left( \frac{0.08}{0.0001891} \right) + (366.496) \left( 0.172 \right) \left( \frac{0.639}{0.0000586} \right) \right]$$

$$\Delta = 0.000447 \text{ m}$$

$$\Delta = 0.45 \text{ mm}$$